Solid-State NMR Study of Paramagnetic Bis(alaninato-$\kappa^2 N,O$)copper(II) and Bis(1-amino(cyclo)alkane-1-carboxylato-$\kappa^2 N,O$)copper(II) Complexes: Reflection of Stereoisomerism and Molecular Mobility in ^{13}C and ^{2}H Fast Magic Angle Spinning Spectra

Gábor Szalontai,*,[†] Róbert Csonka,[†] Gábor Speier,[†] József Kaizer,[†] and Jasmina Sabolović[‡]

[†]Department of Chemistry, Faculty of Engineering, University of Pannonia, Egyetem utca 10, H-8201 Veszprém, Hungary
[‡]Institute for Medical Research and Occupational Health, Ksaverska cesta 2, P.O. Box 291, HR-10001 Zagreb, Croatia

S *Supporting Information*

ABSTRACT: Solid-state stereochemistry and mobility of paramagnetic copper(II) complexes formed by aliphatic amino acids (L-alanine, D,L-alanine, 1-amino-2-methyl-alanine) and 1-amino(cyclo)alkane-1-carboxylic acids (alkane = propane, butane, pentane, hexane) as bidentate ligands has been studied by ^{13}C and ^{2}H solid-state fast magic angle spinning (MAS) NMR spectroscopy. We examined the prospective method to characterize solid-state paramagnetic compounds in a routine way. Both ^{13}C and ^{2}H MAS spectra can distinguish D,L and L,L diastereomers of natural and polydeuterated

Bis([D₆]L-alaninato)copper(II)
²H MAS, rotation 30000 Hz
2nd and 3rd spinning sidebands

bis([D$_n$]alaninato)copper(II) (n = 0, 2, 8) complexes with axial and/or equatorial methyl positions (conformations) primarily due to different Fermi-contact (FC) contributions. The three-bond hyperfine couplings clearly show Karplus-like dependence on the torsional angles which turned out to be a useful assignment aid. Density functional theory calculations of the FC term and crystal structures were also used to aid the final assignments. The correlations obtained for bis(alaninato-$\kappa^2 N,O$)copper(II) complexes were successfully used to characterize other complexes. The usefulness of the ^{2}H MAS spectra of the deuterated complexes was underlined. Even the spectra of the easily exchangeable amine protons contained essential stereochemical information. In the case of a dimer structure of bis(1-aminohexane-1-carboxylato-$\kappa^2 N,O$)copper(II) both the ^{13}C and ^{2}H resolutions were good enough to confirm the presence of the *cis* and *trans* forms in the asymmetric unit. With regard to the internal solid-state motions in the crystal lattice, the obtained quadrupolar tensor parameters were similar for the D,L- and L,L-alaninato isomers and also for the *cis*—*trans* forms suggesting similar crystal packing effects, static amine deuterons involved in hydrogen bonding, and fast rotating methyl groups.
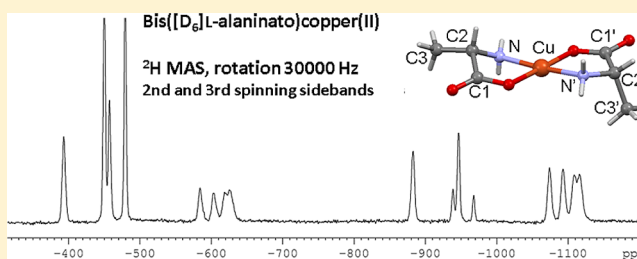
■ INTRODUCTION

Stereochemistry of paramagnetic organometallic complexes formed by bidentate ligands is of general interest both in liquid and solid states. In crystalline solids single-crystal diffraction is the standard method for providing molecular structure. However, NMR has much to offer the chemist because it can both supplement and complement the diffraction results.[1a–c] Unfortunately, NMR spectroscopy of paramagnetic compounds is often elusive as positions of resonances may change unpredictably and signals often broaden beyond detection.[2a–d,3] Thus, information on spectra may remain unexploited. However, a recently proposed solid-state NMR methodology, coined by Ishii and co-workers as very fast magic angle spinning (VFMAS) method,[4–9] promised a breakthrough in such applications, at least for paramagnetic centers possessing a small magnetic susceptibility (electron spin $S = ^1/_2$).[2b] For recording of NMR spectra of systems containing metal ions with larger susceptibilities and with $S > ^1/_2$ these methods have

recently been combined with new pulse schemes utilizing short high-powered adiabatic pulses.[2c,d] Kumara Swarmy et al. have pointed out very recently that nearly complete assignment of a paramagnetic metalorganic system (Cu-Cyclam) can be achieved by dipolar ^{1}H–^{1}H and ^{1}H–^{13}C correlations.[10] We too have recently demonstrated that the combination of ^{13}C and ^{2}H fast-MAS spectra of the crystals of anhydrous *trans* and aqua *cis* bis(L-valinato)copper(II) complexes is indeed a very effective tool for studying conformational disorder and molecular mobility in the solid state.[11] While the easily recordable ^{13}C fast-MAS spectra are informative on the local environment of the nuclei in the crystalline phase (e.g., the spectra provide the number of crystallographically inequivalent nuclei, which can be used in crystallographic space group determination too[1a,b]), the ^{2}H MAS spectroscopy can detect

internal motions present in the crystals.[12,13] In diamagnetic compounds the spectral resolution of the ^{2}H MAS spectroscopy is normally too small to be useful for stereochemical assignments. However, in paramagnetic compounds the enhanced ^{2}H chemical shift dispersion of the nuclei touched by the paramagnetic effects can be huge, and thereby, the spectra simultaneously carry information both on the stereochemistry and the mobility of the molecules.[14−16] It is known that hydrogen bonding is vital in linking molecules into a three-dimensional framework in the crystalline state. The ^{2}H MAS spectra can provide essential information about hydrogen bonds and their strengths. We are going to demonstrate that, for paramagnetic compounds, whenever partially or completely deuterated samples are available, ^{2}H MAS spectroscopy offers a possibility not often exploited so far.

In the present paper we applied the VFMAS method to stereoisomers and geometric isomers of copper(II) amino acid complexes ($S = ^1/_2$) for which experimental crystal and molecular structures have already been reported. The complexes studied were bis(D,L-alaninato-κ^2N,O)copper(II) (**1a**),[17a−d] bis(L-alaninato-κ^2N,O)copper(II) (**1b**),[17a,18a−c] bis-(1-amino-2-methyl-alaninato-κ^2N,O)copper(II) (**2**),[19a,b] and bis(1-amino(cyclo)alkane-1-carboxylato-κ^2N,O)copper(II), where alkane stands for butane (**3**),[20] pentane (**4**)[17a] (Figure 1), and hexane (**5**)[20] (Figure 2). Where available, we also

studied their partially or completely deuterated forms. While in **1a** the methyl carbon atoms adopted the equatorial position in both chelate rings (**ee** conformation), in all **1b** crystal structures the conformation was axial−equatorial (**ae**) (Figure 1).

It is known that the assignment of NMR spectra is notoriously difficult in paramagnetic compounds. To assist signal assignments we have studied the conformation dependence of the hyperfine coupling constants and performed quantum chemical DFT calculations, suggested also by others,[2b,17d,21,22a,b,23a−e,24] to predict the Fermi-contact contributions. In addition, a computational approach was recently recommended to predict also the pseudocontact shift values for the nuclei located in the close vicinity of the unpaired electron by means of the DFT calculated electron probability density, hyperfine tensor, and magnetic susceptibility tensor.[25a] Although the solid-state ^{13}C, ^{1}H,[4,5] and ^{2}H NMR data[14] and computational DFT predictions have already been reported for the trans **1a** hydrate complex,[17d] no such data exist for either trans or cis **1b** complex, apart from the ^{1}H MAS spectrum.[5]

Clearly, further experiments were needed to gain deeper insight into the applicability of this method for stereochemical characterization, so we decided to revisit the alaninato case and carry out a systematic NMR study including D,L (L,D) and L,L (D,D) stereoisomers, cis and trans geometric isomers, and several of their ^{2}H labeled forms. We examined the correlation between the paramagnetic shift and structural features as well as between the ^{2}H quadrupolar tensor anisotropy and molecular mobility (including hydrogen-bonded molecules) in order to apply them for cyclic amino acid complexes whose stereochemistry was determined by X-ray diffraction structural analysis (complexes **2**,[19a,b] **3**,[20] **4**,[17a] and **5**[20]) and IR methods (complexes **2** and **4**).[20]

■ THEORY: EFFECTS OF ELECTRON−NUCLEUS INTERACTIONS ON NMR SPECTRA[2A,B,22A,25A−E,26]

1. Paramagnetic Shift Contributions in Solids. A paramagnetic center interacts with the surrounding nuclear spins and changes the NMR spectrum. The effective field observed by a target nucleus is the following:

$$B_{\text{eff}} = B_{\text{diamagnetic}} + B_{\text{Fermi-contact}} + B_{\text{pseudocontact}} + B_{\text{BMS}}$$

(1)

Of these, the $B_{\text{Fermi-contact}}$ (FC) is often the largest (especially for paramagnetic centers possessing small magnetic susceptibility). It is a scalar coupling type of interaction that depends on the sign and magnitude of the hyperfine coupling constant A, i.e., depends on the number and type of bonds connecting the target nucleus with the unpaired electron. Therefore, like the J couplings, it is a sensitive probe of the stereochemistry too. $A \propto$
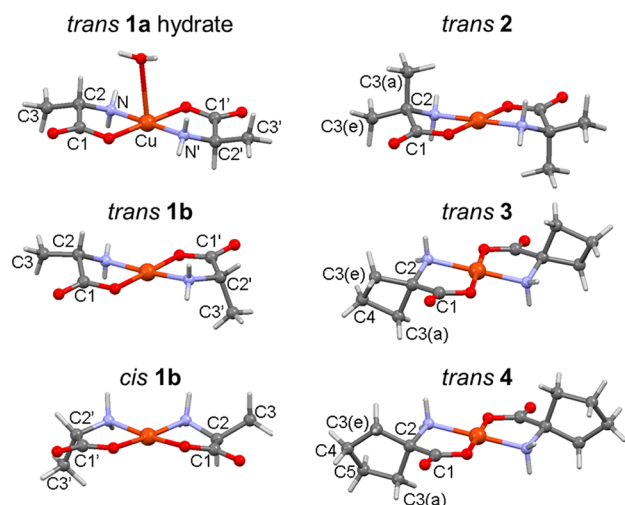

Figure 1. Studied copper(II) amino acidato complexes with known crystal structures (the experimental Cartesian coordinates were used for the drawings). The atom labeling shown was used for monomeric structures throughout this paper. The axial and equatorial positions of the C3 atom are denoted with (a) and (e), respectively.
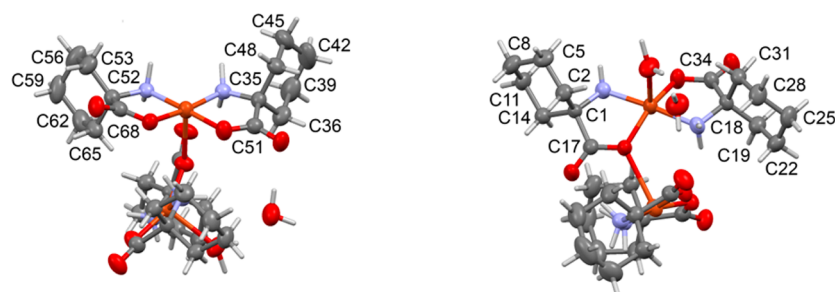

Figure 2. Asymmetry unit of the X-ray crystal structure of **5**.[20] Two views are given for clarity. Left: cis isomer on top. Right: trans isomer on top. The atom numbering used here was taken from the crystal structure and is different from the one used for monomer complexes.

$\gamma_I g_e \beta_e |\Psi|^2$, where γ_I is the nuclear gyromagnetic ratio, $g_e \approx 2.003$ is the free electron g-value, β_e is the Bohr magneton, and $|\Psi|^2$ denotes the electron spin density at the nucleus. A is expressed in J or in Hz (it changes sign and is on the MHz scale). The Fermi-contact shift, δ_{FC}, is isotropic and temperature dependent $(1/T)$. Its contribution can be neglected at electron–nucleus distances larger than 5 Å. For polycrystalline solids undergoing MAS, δ_{FC} is given by (ref 2a)

$$\delta_{FC} = \frac{A}{\hbar} \frac{\overline{g} \beta_e S(S+1)}{3\gamma_I kT} \quad (A \ll g_e \beta_e B_o) \tag{2}$$

where k is the Boltzmann constant, $\hbar$ is the Planck constant divided by 2π, B_o is the external magnetic field, T is the temperature, $\overline{g} = (g_{xx} + g_{yy} + g_{zz})/3$ is the average of the principal components of the electron **g**-tensor, and S is the spin angular momentum of the electron.

The $B_{pseudocontact}$ (PCS) interaction is of much smaller magnitude (on the order of a few to tens of ppm) but is of special interest because it is a direct electron/nucleus dipolar effect. As such, it depends on the distance between the target nucleus and the unpaired electron. The pseudocontact shift can take on positive or negative values. Its isotropic part is nil if the magnetic susceptibility tensor of the paramagnetic center is isotropic. In the cases of Cu^{2+}, Mn^{2+}, and Gd^{3+} ions the anisotropy of the magnetic susceptibility tensor is generally small. Its anisotropic part [removable by MAS and temperature dependent $(1/T)$] can be readily detected since it causes a spinning sideband manifold. This anisotropy, Δ_{aniso}, is related to the distance, r, between the target nucleus and the unpaired electron (r^{-3}). The pseudocontact shift is conveniently expressed in terms of a magnetic susceptibility tensor, χ, the principal component of which is related to the principal components of **g**, the electron **g**-tensor:[2a]

$$\chi_{ii} = \mu_o \beta_e^2 g_{ii}^2 \frac{S(S+1)}{3kT} \tag{3}$$

where $ii = xx$, yy, or zz, and μ_o is the magnetic permeability of the free space. Under rapid MAS conditions the PCS contribution is given by eq 4:[2a]

$$\delta^{PCS} = \frac{1}{12\pi r^3}\left[\Delta\chi_{ax}(3\cos^2\theta - 1) + \frac{3}{2}\Delta\chi_{rh}\sin^2\theta\cos 2\varphi\right] \tag{4}$$

where r is the electron–nucleus distance, θ and φ are the polar and azimuthal angles, respectively, describing the orientation of the electron–nucleus vector in the principal axis frame of the susceptibility tensor. The axial and rhombic components of the susceptibility tensor are given by

$$\Delta\chi_{ax} = \chi_{zz} - \frac{\chi_{xx} + \chi_{yy}}{2} \tag{5}$$

$$\Delta\chi_{rh} = \chi_{xx} - \chi_{yy} \tag{6}$$

B_{BMS} describes the bulk magnetic susceptibility contribution.[27] It is a demagnetization field which, like the PCS term, is orientation-dependent and may produce shift and broadening of the resonance lines. In principle it can be quite large, especially for paramagnetic centers featuring a large spin ($S > 1/2$);[2b] however, it is generally ignored in structural NMR studies of electron spin $S = 1/2$ cases, such as Cu(II).

2. Paramagnetic Relaxation Enhancements (PREs). One should consider five independent relaxation rates when investigating the relaxation of $I = 1$ nuclei, that is, two spin–lattice [R_{1z} (return of the Zeeman energy to its equilibrium value) and R_{1Q} (decay of the quadrupolar energy)] and three spin–spin relaxation times.[28] Measurements of R_{1z} and R_{1Q} are particularly useful since they are very sensitive to molecular motions.

In paramagnetic solids the Solomon dipolar relaxation rate (SL), $R_{1,2}^{SL}$, which originates from the modulation of the electron–nucleus dipolar relaxation,[29a,b] is the main source of PRE. Since R_2^{SL} is proportional to the square of the gyromagnetic ratio of the nucleus, γ_I, ^{13}C or ^{15}N signals may be observable even if ^1H signals are very broad. The Curie relaxation mechanism, often dominant in solutions, is practically absent in the solid state.[29c,d]

As demonstrated earlier by the Ishii's group,[7−9] important structural information such as absolute and relative electron–nucleus distances is also available from the ^{13}C spectra, but these are beyond the scope of this Article.

■ EXPERIMENTAL SECTION

1. Sample Preparations. We synthesized copper(II) amino acidates and prepared single crystals by following the published procedures for *trans* **1a** hydrate,[17c] *trans* **1b**,[30] and **3**.[20] All other complexes were synthesized as described for **3**.[20]

2. NMR Spectroscopy. All solid-state NMR spectra were recorded on a Bruker Avance II spectrometer with proton frequency of 400.13 MHz (9.38 T) equipped with a 2.5 mm CPMAS probe. There were 8−12 mg polycrystalline samples used to fill up the Zirkonia rotors. The ^{13}C spectra (100.61 MHz) were recorded under proton decoupling; without ^1H decoupling, the spectra were somewhat inferior. At 20 kHz rotation the lines are still about 20% broader, relative to those obtained with ^1H decoupling. Several strengths for the decoupling rf field were tried, but practically no change was observed between 150 and 75 kHz; however, below that the line broadening sets in. No decoupling was applied in the case of the ^2H spectra (61.42 MHz). The typical relaxation delay and acquisition times were 200 ms and 0.005 s, respectively, enabling extremely fast signal accumulation. α-Glycine was used as an external reference for the ^{13}C spectra ($\delta_{C=O}$ 176.5 ppm). All spectra were recorded at ambient temperature (~300 K) without regulation. The actual temperature of the samples was estimated by using a calibration curve obtained for external $PbNO_3$. At 20 kHz rotation the temperature increase due to the frictional heat of the bearing gas was ≤10 K.

For the measurements we have used the following standard NMR methods (Bruker BioSpin Topspin 2.1.3.): fast-MAS (≥20 kHz); rotor-synchronized Hahn-echo[13] under fast-MAS (rotation ≥20 kHz) condition; cross-polarization magic angle spinning (CPMAS)[31] (rotation range 11−24 kHz); cross-polarization−polarization inversion (CPPI)[32] under fast-MAS (rotation >15 kHz). For ^2H spectra we found that by careful calibration of the preacquisition delay the simple direct excitation sequence provides spectra comparable to those obtained using the solid-echo scheme. Experimental ^2H MAS NMR spectra were simulated using the Bruker Solid State Analysis Software (Topspin 2.1.3.).[33] It simulates the spinning sidebands (SSBs) for the first-order quadrupolar interaction of all transitions. The Haeberlen notation[12] was used to describe the chemical shift anisotropy (CSA) and quadrupolar tensors. The assumed motional models were also checked by simulations using the NMR-WEBLAB package.[34]

It was found that by repeated slow crystallization the attainable spectral resolution could be improved.

3. Quantum Chemical Calculations. As already stated, the hyperfine coupling constant A (eq 2) is proportional to the electron spin density at the nucleus, $|\Psi|^2$. The spin density can be obtained from quantum chemical calculations by means of the spin-up and spin-down molecular orbitals, i.e., the difference in the α and β spin densities at the nucleus, $\rho_{\alpha\beta}$[23a]

Table 1. Experimental ¹³C NMR Chemical Shifts (δ_P's), Calculated DFT/B3LYP ¹³C FC Shifts (δ_{FC}^{calcd}'s), Diamagnetic Shifts (δ_{dia}^{calcd}'s), and Chemical Shifts (δ^{calcd}'s, $\delta_{complex}^{calcd}$'s) of the Studied Copper(II) Complexes, and Experimental Solid-State ¹³C Diamagnetic Shifts (δ_{dia}) of Their Corresponding Free Ligands (FLs)[a]

¹³C	δ_{dia} (FL)	δ_{dia}^{calcd}	δ_P	δ_{FC}^{calcd}	δ^{calcd}	$\delta_{complex}^{calcd}$
			1a *trans*			
C1,1'	177.4	175.4	−209.6	−469	−292	−294
C2,2'	50.3	47.0	−290.2	−374	−324	−327
C3,3'	19.5	0.2	177.9 (e)	176 (e)	196 (e)	176 (e)
			1a *cis*[b]			
C1,1'	177.4	176.0	−207.0	−483, −479	−306, −302	−307, −303
C2,2'	50.3	53.3	−305.0	−397, −392	−347, −342	−344, −339
C3,3'	19.5	22.8	19.3 (a), 233.5 (e)	−16 (a), −16 (a)	4 (a), 4 (a)	7 (a), 7 (a)
			1b *trans*			
C1,1'	177.4	174.8, 181.4	−205.5	−489, −423	−312, −246	−315, −245
C2,2'	50.3	43.0, 42.9	−296.1, 312.9	−391, −351	−341, −301	−338, −308
C3,3'	19.5	−7.7 (a), −7.1 (e)	18.0 (a), 240.1 (e)	−11 (a), 264 (e)	9 (a), 284 (e)	−19 (a), 257 (e)
			1b *cis*[c]			
C1,1'	177.4	174.0, 178.3		−444, −364	−267, −187	−270, −186
C2,2'	50.3	53.3, 54.7		−444, −376	−394, −326	−391, −321
C3,3'	19.5	19.4 (a), 19.2 (e)		−6 (a), 162 (e)	14 (a), 182 (e)	13 (a), 181 (e)
			2			
C1,1'	178.3	179.1	−208.0	−464	−286	−285
C2,2'	59.4	62.6	−276.1	−391	−332	−328
C3,3'	24.1 (a), 22.0 (e)	27.3 (a), 26.1 (e)	34.3 (a), 232.5 (e)	−4 (a), 256 (e)	20 (a), 278 (e)	23 (a), 282 (e)
			3[d]			
C1,1'	178.0	181.1	−241.1	−483	−305	−302
C2,2'	58.7	56.7	−306.1	−421	−362	−364
C3,3'	31.2 (a), 29.8 (e)	−8.0 (a), 12.4 (e)	34.6 (a), 243.4 (e)	8 (a), 202 (e)	39 (a), 232 (e)	0 (a), 214 (e)
C4,4'	16.5	15.8	61.8	8	25	24
			4[e]			
C1,1'	178.6	179.6	−239.5	−491	−312	−311
C2,2'	69.1	71.0	−275.8	−389	−320	−318
C3,3'	38.0 (a), 38.0 (e)	27.5 (a), 21.9 (e)	41.3 (a), 199.0 (e)	−19 (a), 129 (e)	19 (a), 167 (e)	9 (a), 151 (e)
C4,4'	23.3	4.8	22.7	−15	8	−10
C5,5'	23.3	6.5	30.9	−7	16	−1

[a]The chemical shifts are expressed in ppm. The experimental δ_P values are referred to external α-glycine (C=O = 176.5 ppm). The axial and equatorial C3,3' positions are denoted with (a) and (e), respectively (Figure 1). The calculated chemical shifts are defined in eqs 9–11. [b]The δ_P dominant signal C3 (a) (Figure 3, bottom) is assigned to *cis* **1a** with the **aa** conformation, and the minor C3' (e) signal is assigned to the mixture of all possible *cis* conformers with the equatorial C3' position. The δ_{FC}^{calcd} and δ_{dia}^{calcd} are calculated for a predicted crystal structure of *cis* **1a** hydrate with the **aa** conformation (Supporting Information Figure S9). [c]For *cis* **1b** only the calculated ¹³C chemical shifts are available (the DFT/B3LYP calculations were based on a previously reported experimental crystal structure[18c]). [d]δ_{dia} (FL) values are the average of two polymorphs. [e]δ_{dia} (FL) values are a tentative assignment.

$$\rho_{\alpha\beta} = \sum_{i}^{occ} \left[|\Psi_i^-(0)|^2 - |\Psi_i^+(0)|^2 \right] \qquad (7)$$

where i goes over all occupied molecular orbitals and is calculated at the position of a target nucleus. The calculated value of the FC hyperfine shift, δ_{FC}^{calcd}, was estimated using eq 9, which is obtained by substituting eq 8 for the hyperfine coupling constant A into eq 2:[23a]

$$A = \frac{\mu_0 \hbar \gamma_K g_e \beta_e}{3S} \rho_{\alpha\beta} \qquad (8)$$

$$\delta_{FC}^{calcd} = \frac{\mu_0 \beta_e^2 g_e^2 (S+1)}{9kT} \rho_{\alpha\beta} \qquad (9)$$

Here S stands for the electronic spin state of the studied copper(II) systems ($^1/_2$), T is the temperature, and the other physical constants have their usual meaning.

To calculate the spin densities at the ¹³C and ¹H nuclei in *trans* **1a** hydrate, *cis* **1a** hydrate, *trans* and *cis* **1b**, *trans* **2**, *trans* **3**, *trans* **4**, and the *trans–cis* dimeric **5** in the solid state, we applied the cluster approach[24] in which the central metal complex was surrounded with a number of closest complexes from a crystal structure. The cluster models were constructed for all of the studied compounds from their experimental crystal structures, except for *cis* **1a** because there is no reported molecular and crystal structure for that stereoisomer. Instead, a cluster model was built from a predicted crystal structure of *cis* **1a** hydrate, which is described in the Supporting Information (Figure S9). The DFT method with the unrestricted B3LYP hybrid density functional[35a–d] was used for the calculations with the following basis set combination:[17d,23a] a Wachters' basis (62111111/3311111/3111) for Cu,[35e] 6-311G* for other heavy atoms, 6-31G for hydrogen atoms of the central cluster unit, and 3-21G* for the noncentral cluster-unit atoms. The choice of the functional/basis set used is based on the study of Oldfield and co-workers on the principal electronic interactions in the solid-state MAS NMR shifts of *trans* **1a** hydrate clusters.[17d] The calculation and result details for the cluster systems are given in the Supporting Information.

If PCS and BMS terms (eq 1) can be neglected, then the ¹³C NMR hyperfine shift can be solely related with the diamagnetic and FC terms.[2b] DFT/B3LYP ¹³C NMR isotropic shielding constants, σ_{iso}, were calculated using the gauge-including atomic orbitals (GIAO) method[35f] for the molecular structures of the studied complexes taken from their experimental and predicted crystal structures. The ¹³C diamagnetic shift, δ_{dia}^{calcd}, was accounted for using eq 10:
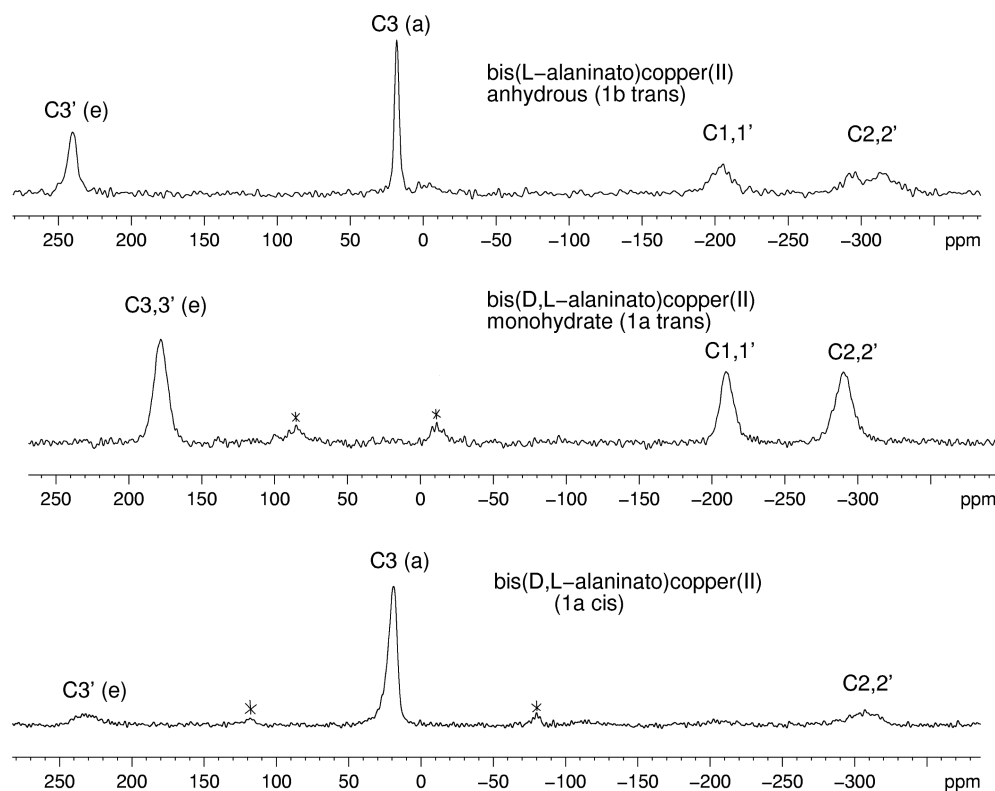
Figure 3. 100.61 MHz solid-state ^{13}C fast-MAS and CPMAS spectra of different bis(alaninato)copper(II) complexes. Top: rotor-synchronized Hahn-echo spectrum of the anhydrous *trans* **1b**. Middle: Hahn-echo spectrum of *trans* **1a**. Bottom: CPMAS of suspected *cis* isomer *cis* **1a** (or mixture of *cis* isomers) prepared using D,L-alanine as ligand. Note that, using CPMAS, signals of C1,1′ are missing from the spectrum. Asterisks indicate spinning sidebands. The axial and equatorial C3,3′ positions are denoted with (a) and (e), respectively.

$$\delta_{dia}^{calcd} = \sigma_{ref} - \sigma_{iso} \tag{10}$$

Here, σ_{ref} is the calculated reference isotropic ^{13}C magnetic shielding in tetramethylsilane (183.3 ppm).[11] For spectra signal assignment purposes, we evaluated the reproduction of the observed hyperfine chemical shifts δ_P's with the calculated δ^{calcd} and $\delta_{complex}^{calcd}$:

$$\delta^{calcd} = \delta_{FC}^{calcd} + \delta_{dia} \tag{11a}$$

$$\delta_{complex}^{calcd} = \delta_{FC}^{calcd} + \delta_{dia}^{calcd} \tag{11b}$$

In eq 11a, δ_{dia} stands for the experimental solid-state ^{13}C diamagnetic shifts of the complexes' corresponding free ligands. The evaluation was motivated by the fact that, for the bis(L-valinato)-copper(II) complexes, the measured δ_{dia} values for the L-valine crystalline sample reproduced the measured hyperfine chemical shift better than the DFT/B3LYP δ_{dia}^{calcd} values did.[11]

The same density functional/basis set was used for the calculations of the equilibrium structures and relative energies of the *trans* and *cis* **aa**, **ae**, and **ee** conformers of **1a** and **1b** stereoisomers in the gas phase, and in the water medium within the polarized continuum model (PCM) approximation. The PCM of Tomasi and co-workers,[36a] modified by Barone and co-workers,[36b] was used to describe the effects of the aqueous medium in the self-consistent reaction field calculations. The environmental temperature was set to 300 K. The water solvent was specified by the dielectric constant of 78.39. The united-atom topological model was applied to solvent radii optimized for the PBE0/6-31G(d) level of theory.[36c−e] The DFT/B3LYP calculations were performed with the Gaussian 03 program package.[37]

■ RESULTS AND DISCUSSION

1. Stereochemistry of Bis(alaninato)copper(II) Complexes Based on ^{13}C Very Fast-MAS and CPMAS Spectra. Prediction of the paramagnetic shifts is difficult, especially in

case of heteroatoms.[2] In copper(II) complexes the FC contribution is expected to dominate the spectra. As mentioned, FC changes as the sign and magnitude of the hyperfine coupling constant A change. For instance, in aliphatic amino acidates the signals of carbon atoms two bonds away from the copper (C1,1′ and C2,2′ in Figure 1) are low-frequency shifted ($A/\hbar$ is negative) and may broaden beyond detection; carbon atoms three bonds away (e.g., C3,3′) are high-frequency shifted ($A/\hbar$ is positive), and are, normally, clearly visible.[2] No clear trend was observed for carbons more than three bonds away from the paramagnetic center, and the effect attenuated rapidly. Though in a complicated manner, the three-bond hyperfine couplings depend also on the relative positions of the unpaired electron density and the target nucleus. Thereby the D,L and L,L isomers, representing **ee** and **ae** methyl configurations in the complexes studied, can, probably, be distinguished.

Concerning the experimental crystal structures available in the literature, there are several reported X-ray crystal structure redefinements of the same crystal modification for *trans* **1b** (space group $P2_1$, **ae** conformation),[17a,18a,b] *trans* **1a** hydrate (space group $C2/c$, **ee** conformation),[17a−d] and two neutron diffraction crystal structures of *cis* **1b** (measured at 7 K and room temperature; space group $P2_12_12_1$, **ae** conformation).[18c] These single-crystal structures served as references for the copper−carbon and copper−deuteron distances, valence, and dihedral angles (assuming that Cu···D and Cu−N−D can be approximated with the corresponding Cu···H and Cu−N−H values). The structure of microcrystals used in the NMR measurements was generally assumed to be identical to that of the single crystals used for diffraction measurements.

1.1. Distinction of D,L (L,D) and L,L (D,D) Isomers of Bis(alaninato)copper(II) Complexes. We have collected the measured and calculated chemical shifts in Table 1. The ^{13}C MAS and CPMAS spectra of the available isomers (D,L-*cis* and D,L-*trans*; and D,L-*trans*) are compared in Figure 3.

1.1.1. trans 1a Hydrate. The reported X-ray structure is a 1D polymer with water−Cu chains, and these chains are connected by a large 3D hydrogen-bond network.[17a−d] In this form both methyl groups take equatorial position (**ee**). The solid-state ^{13}C MAS spectrum (Figure 1, middle) indicates only three crystallographically inequivalent carbon sites, i.e., a 2-fold symmetry.[21] Thus, either a proper C_2 axis and/or a center of inversion must exist.[38] Therefore, assignment of the spectrum was relatively straightforward. With the help of CPMAS spectra[31] the C1,1′ and C2,2′ carbons could be distinguished and assigned to the signals at −209.6 and −290.2 ppm, respectively. More subtle was the interpretation of the +177.9 ppm shift. With the assumption that our crystals were identical to the single crystal from which the X-ray structure was solved,[17a] this chemical shift should correspond to the equatorial methyl position. DFT/B3LYP calculations of ^{13}C and ^{1}H NMR chemical shifts confirmed the assignment of the +177.9 ppm signal to the equatorial position.[17d]

1.1.2. Anhydrous 1b Isomers. The reported X-ray structures[17a,18a−c] show anhydrous complexes in either *trans* or *cis* configuration but always with (**ae**) arrangement of the methyls. In agreement with such conformation, the ^{13}C MAS spectrum of the L,L isomer showed six different carbon sites (Figure 3, top, and Table 1). The broad signal at −205.5 ppm was assigned to the carbon of the coordinated C=O (C1,1′) groups (again by CPMAS experiments where the contact time was systematically changed). Thus, the two slightly overlapping broad signals at −296.1 and −312.9 ppm could be assigned to the C2,2′ methine carbons.

Concerning the +240.1 and +18.0 ppm signals, CPPI spectra[32] with different repolarization times did not reveal any difference between the spin dynamics of these signals suggesting that both should belong to the same type of CH$_n$ carbons (C3 and C3′ methyls). Although the +240.1 ppm signal was closer to the equatorial signal of the D,L isomer (+177.9 ppm), its assignment to the equatorial position was still problematic. Interpretation of the size of the FC contribution to the equatorial and axial methyl positions was attempted by assuming Karplus-like[39,40] behavior of the three-bond contact hyperfine coupling. The available X-ray structures all show Cu−N−C2−C3 torsional angle values, θ, in the range 90°−100° for the axial C3′ carbons and 170 ± 5° for the equatorial C3 carbons. According to the general Karplus equation ($\cos^2\theta$ dependence) the FC contribution will show a minimum at about 90° of the Cu−N−C2−C3 torsional angle.

DFT/B3LYP calculations of the FC contributions (Table 1) gave the predicted shifts for carbons C1,1′ and C2,2′ in the right range, but the deviations from the experimental values were occasionally too great, and therefore useless for stereochemical assignment. At the same time, we obtained very good correlation between the experimental δ_P and calculated δ^{calcd} and $\delta^{calcd}_{complex}$ values (Table 1 and Supporting Information Figure S10). The measured δ_P values were better reproduced by means of δ^{calcd}_{dia} than δ^{calcd}_{dia} (i.e., the regression coefficient $R = 0.98$ for δ^{calcd} and $R = 0.97$ for $\delta^{calcd}_{complex}$, the regression line slope was 1.1 ppm in both cases, and the intercept was −15.9 and −30.2 ppm for δ^{calcd} and $\delta^{calcd}_{complex}$, respectively; Supporting Information Figure S10). Like for

bis(L-valinato)copper(II),[11] this finding suggests that when the complexes' diamagnetic analogues are unavailable, the ^{13}C diamagnetic shifts measured for polycrystalline free ligands can serve as a suitable approximation to the diamagnetic reference (bearing in mind that Cu^{2+} is a relaxation reagent rather than a shift agent) for signal assignment purposes. DFT/B3LYP calculations using the clusters of 21-Cu supermolecular assemblies to mimic the solid phase for the *trans* L,L isomer predicted +284 and +9 ppm values (Table 1) for the equatorial and axial C3 methyls, respectively. On the basis of these data and also on the spectral analogy with the symmetric D,L-isomer, the signal at +240.1 ppm was assigned to the equatorial position (Table 1).

1.2. Distinction and Assignment of the cis−trans Geometric Isomers (Coordination Modes) of the Bis(alaninato)-copper(II) Complexes. As mentioned, single-crystal X-ray structures[18a−c] confirmed the crystallization of both *cis* and *trans* bis(alaninato)copper(II). The distinction of these geometric isomers on the basis of their ^{13}C MAS spectra should be straightforward, but the assignment of signals to a particular isomer is ambiguous. IR spectroscopy, widely used for this purpose for a long time,[41] suffers from the same limitation. The distinction ability of EPR spectroscopy, similar to that of NMR spectroscopy, depends on the sensitivity of hyperfine coupling constants A to the coordination mode.[42]

In the *cis* and *trans* isomers the copper−carbon and copper−proton (deuteron) distances are practically identical; the small PCS term, though it depends also on the orientation of the dipolar coupling vector relative to the susceptibility tensor (eq 4), is probably useless for distinction purposes, even if we could separate it from other contributions. At first sight, significant *cis−trans* differences of the FC contributions may be expected, as they were observed for the bis(L-valinato)copper(II) complexes.[11] Namely, in the *cis* and *trans* forms the bond-weakening "*trans* effect" of the coordinating groups[43] is different, and may result in different hyperfine coupling values. However, the experimental Cu−N and Cu−O distances found in the *cis* (**ae**)[18c] and *trans* (**ee**)[17a−d] and *trans* (**ae**)[17a,18a,b] isomers did not show remarkable deviations. Unfortunately, we did not have either (**ee**) or (**ae**) *cis/trans* sample pairs to separate the *cis/trans* coordination effect from the effect of the axial/equatorial methyl substitution on C2 and C2′.

Whenever we followed the synthesis method suggested for the preparation of the *trans* D,L isomer by O'Brien,[17e] the spectrum of the resulting blue powder looked like the one shown at the bottom of Figure 1. Surprisingly, apart from the increased line widths of the signals, it was rather similar to the spectrum of the L,L-isomer (Figure 1, top); i.e., it exhibited, though minor and broad, an "equatorial" (∼ +235 ppm) and a dominant "axial" (∼ +20 ppm) methyl signal (Figure 1, bottom). Recrystallization of this powder from H$_2$O or from D$_2$O resulted in the middle spectrum in Figure 1, i.e., that of the already known symmetric *trans* monohydrate D,L complex. The phenomenon and the dominant signal can be explained by immediate formation of a *cis* D,L isomer in an (**aa**) conformation and with C_2 symmetry (Supporting Information Figure S9, Table 1, and Supporting Information Table S1). Additionally, all possible variants arising from the racemic D,L ligand, i.e., the L,L, D,D, D,L stereoisomers, could be credited for the appearance of signals both in the "equatorial" and in the "axial" regions.

DFT/B3LYP calculations of the FC contributions, δ^{calcd}_{FC}, predict that shifts of C3 (**e**) of the *trans* and *cis* isomers of **1b**
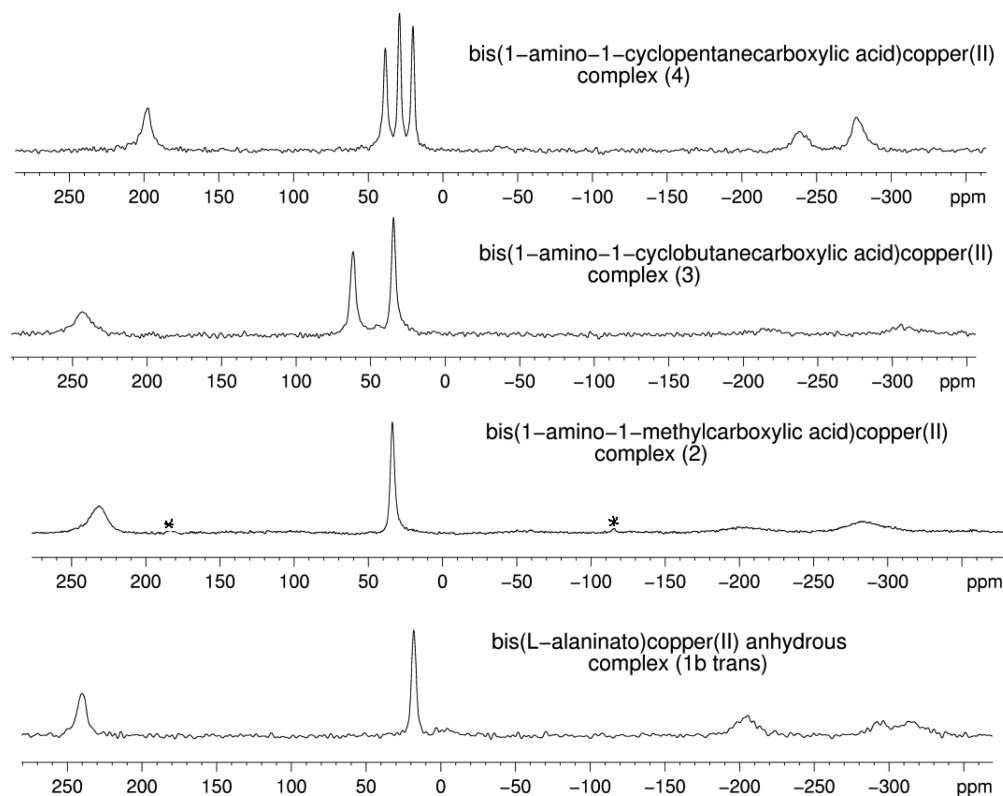
Figure 4. Comparison of solid-state ^{13}C MAS rotor-synchronized Hahn-echo spectra of complexes *trans* **1b**, **2**, **3**, and **4**. Asterisks indicate spinning sidebands. Larmor frequency 100.61 MHz, rotation 20 kHz, temperature 300 K.

may differ by 102 ppm (Table 1). At the same time the shifts predicted for the C3′ (**a**) carbons practically do not differ (Table 1).

The DFT/B3LYP calculated energy difference between each of the *trans* and *cis* group of **aa**, **ee**, and **ea** conformers of **1a** and **1b** was up to 5.9 kJ mol^{-1} in the gas phase (Supporting Information Table S4). While the *trans* **ee** conformers are more stable than the *cis* **ee** ones by 50.4 kJ mol^{-1} in the vacuum, these energy differences drop significantly to 4.2 and 3.8 kJ mol^{-1} for the L,L (**1b**) and D,L (**1a**) isomer, respectively, in the aqueous solution according to the PCM calculations. The maximum relative energy between the *trans* L,L **ee** and *cis* D,L **aa** conformers in the vacuum (56.3 kJ mol^{-1}) dropped to 10.6 kJ mol^{-1} in the water medium. The energy drop can be explained by more favorable intermolecular interactions with water molecules and *cis* isomers as compared the same interactions with *trans* isomers.[44a−c] Relatively small energy differences may suggest the presence of all 12 conformers in aqueous solution at room temperature. This suggests that the domination of the *cis* isomer in the initially synthesized powder may be owed to a kinetically driven crystallization. On the other hand, the available chemical evidence reveals that the anhydrous *trans* L,L and aqua *trans* D,L isomers recrystallized from the aqueous solution by slow evaporation at room temperature may be influenced by both thermodynamic and kinetic factors. Apart from that, the formation of the **ae** and **ee** conformations in their crystal structures may be affected by the crystal packing effects.

2. ^{13}C MAS Study of Bis(1-amino(cyclo)alkane-1-carboxylato-κ^2N,O)copper(II) Complexes. In bis(1-amino-(cyclo)alkane-1-carboxylato-κ^2N,O)copper(II) complexes the size of the C2 attached cycloalkane ring is increasing stepwise (Figure 1), which makes easy following of the spectral changes

in relation to the information obtained from **1a** and **1b** possible. The cycloalkane ring reduces the conformational mobility of the chelate ring, so similar stereochemistry is expected for all complexes. The ^{13}C MAS spectra of the anhydrous *trans* **1b**, **2**, **3**, and **4** are compared in Figure 4. Given the ambiguity of the assignment of **1b** discussed above, this compound may serve as reference as it has both axial and equatorial methyl groups attached to the C2 carbon (Figure 1). The available chemical shifts are given in Table 1.

2.1. Complex 2. The single-crystal structure[19a,b] proves that there is a center of inversion between the ligands. Not surprisingly the basic features of the spectrum were rather similar to that of **1b** (Figure 4, bottom). Note that in **2** C3 (**a**) and C3 (**e**) of the same ligand (Figure 1) can produce a spectrum similar to that of *trans* **1b**. The FC and the PCS contributions may be very similar independent of the fact that C3 (**e**) and C3′ (**a**) in *trans* **1b** belong to different ligands (Figure 1).

The signal at 34.3 ppm, being very close to the axial methyl signal of **1b**, was preliminarily assigned to the axial position. At the same time, as indicated by the presence of spinning sidebands, its dipolar anisotropy was much larger in comparison with that of the 232.5 ppm signal. The DFT/B3LYP δ^{calcd} prediction was 20 and 278 ppm for C3 (**a**) and (**e**), respectively (Table 1).

While the large positive paramagnetic shift ($\sim$ +230 ppm) implies a large positive hyperfine coupling value for C3 (**e**), the practically unchanged (almost diamagnetic) position of C3 (**a**) (+34.3 ppm) indicates a much smaller hyperfine contribution. Since the dominant two-bond FC contribution is the largest for the C1,1′ and C2,2′ carbons their assignments are more or less evident. Thus, the broad signals at −202.6 and −283.1 ppm
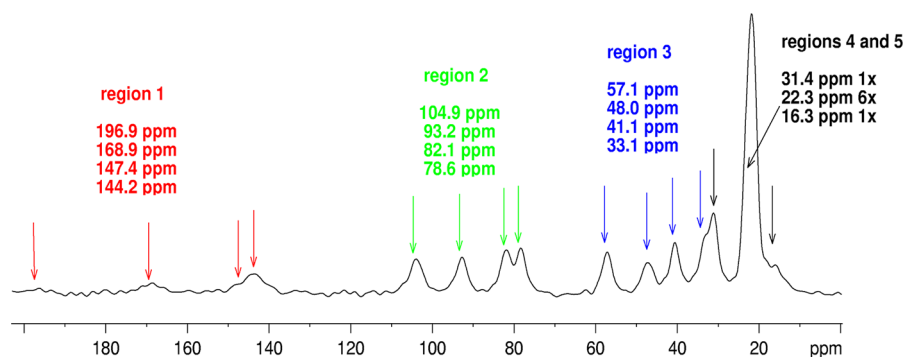
Figure 5. ^{13}C CPMAS spectrum of complex **5**. Only the central part is shown where carbons three and more bonds away from the paramagnetic center give rise to signals. Signals in the indicated regions, four in each, are thought to belong to a specific group of atoms (possessing three- and four-bond hyperfine couplings to the copper), e.g., to that of the equatorial C_β carbons in the red and the axial ones in the black regions. The green and blue regions (2 and 3) are assigned to the four-bond hyperfine couplings. Larmor frequency 100.61 MHz, rotation 10 kHz, temperature 300 K.

were assigned to the carbonyl (C1,1′) and methine (C2,2′) carbons, respectively. With regard to the overall stereochemistry, our conclusion was the following: *trans* complex with a symmetry element and C3 atoms in the equatorial and axial positions.

2.2. Complex 3. In comparison to the spectra of **2**, one more signal was seen at 61.8 ppm (Figure 4, Table 1), as expected. The new signal was assigned to the C4 methylene carbon (Figure 1). Its moderate high-frequency shift is caused by the interplay of the five-bond Cu−O−C1−C2−C3−C4 and four-bond Cu−N−C2−C3−C4 hyperfine couplings. Our conclusion on the stereochemistry was the following: *trans* coordination mode with a center of inversion (Cu), and axial−equatorial arrangement for the C3 (a) and (e) methylenes bound to C2 atom of the cyclobutane ring in agreement with the single-crystal X-ray structure[20] (Figure 1).

2.3. Complex 4. In comparison to the spectra for **3** (Figure 4), one more "diamagnetic" signal appeared at 22.7 ppm. It could belong to either C4 or C5; the DFT/B3LYP results suggest that it belongs to C4 (Table 1). In addition, small changes of other "paramagnetic" signals [C1, C2, C3(a), and C3(e)] were seen (Figure 4), suggesting the same *trans*-N$_2$O$_2$ coordination configuration and the presence of a center of inversion as already seen in **2** and **3**. The X-ray structure[17a] confirmed this prediction.

2.4. Complex 5. We knew from the X-ray structure[20] that we faced a dimer composed of one *trans* and one *cis* aqua complex (Figure 2). The dimer was formed by coordination of a carbonyl oxygen of the *cis* isomer to the Cu atom of the *trans* isomer in apical position.[20] The fact that this compound has two paramagnetic centers has several consequences on the spectral appearance and assignments. Namely, in the ^{13}C CPMAS spectrum (Figure 5), apart from the hardly detectable carbonyl (C1,1′) and C2 and C2′ carbons, 20, partly unresolved, protonated carbon signals were observed in the region from +200 to +10 ppm. That is exactly the number we expected for the four different cyclohexyl groups. This confirms the presence of two different bis complexes in the asymmetric unit, and the C_1 symmetry of the dimer. Starting from the high frequencies (Figure 5), one can further divide the spectrum into four subregions. The first three contain four signals each, and the fourth contains eight signals. We attempted to assign these groups to specific groups of carbons, such as "axial" and "equatorial" C_β atoms two bonds away from Cu. Note that in the cyclohexane rings the stereochemistry of these C_β cannot

be properly described as axial or equatorial; however, as their Cu−N−C2−C$_\beta$ dihedral angles, θ, do differ significantly, we keep the axial−equatorial notation for clarity reasons.

To be able to make a tentative assignment we made use of the dihedral angle dependence of the dominating three-bond FC term confirmed earlier in alaninato complexes (see above). A fairly linear correlation was found between the estimated FC contributions ($\delta_{FC} = \delta_P − \delta_{dia}$) and $\cos^2 \theta$ (Supporting Information Figure S11). On this basis the suspected equatorial and axial C_β signals (Figure 2; *trans* isomer, C14, C19, C31, C2; and *cis* isomer, C53, C65, C36, C48) are most likely found in the red and black regions, respectively. As indicated by DFT calculations (Supporting Information Table S3) the suspected C_γ carbons (see C5, C22, C11, C28, C39, C62, C45, C56 in Figure 2, here four-bond hyperfine couplings are involved) are probably found in the green and blue regions. Signals of all C_δ (C8, C25, C42, C59 in Figure 2, five bonds away from Cu) are buried under the broad singlet at about 22 ppm. Assignment of the signals to the *trans* and *cis* isomer was not possible. Note that in this case both Cu atoms can produce unpaired electron densities on several carbon atoms of both complexes, which can add to the complexity of the problem.

3. Study of Stereochemistry and Solid-State Mobility of the Bis([D$_n$]amino acidato)copper(II) Complexes As Reflected in ^{2}H Fast-MAS Spectra. *3.1. General Features of ^{2}H MAS Spectroscopy.* ^{1}H MAS spectra for hydrous D,L and anhydrous L,L (D,D) alaninato complexes were reported by Ishii et al.[5] Even though this nucleus promises high sensitivity, the recording of high-resolution ^{1}H MAS spectra requires extremely fast sample rotation (≥60 kHz) combined with special NMR methodology.[45a,b] A comparison between the ^{1}H and ^{2}H MAS spectra of **1b** is given in Supporting Information Figure S8.

^{2}H MAS spectroscopy is a generally accepted method for studying motions in the solid state of labeled diamagnetic compounds.[16,28] This is because even small modulation (motions on the microsecond to nanosecond time scale) of a large effect (namely, the quadrupolar coupling C_Q) can more easily be detected. In paramagnetic solids, like the diamagnetic cases, the centerband positions give the isotropic values, and the spectra are characterized by a large number of quadrupolar spinning sidebands. The ^{2}H line shape depends also on the geometry of the motional process;[46] thus, motional models can be validated and identified by simulations of the experimental spectra.[34] Dipolar couplings, rotation speed, temperature, and

mutual orientation of the quadrupolar and dipolar tensors influence the spectra.[15] The strength of the electron−nucleus dipolar interaction affects the extent of asymmetry of the quadrupolar line shape, and also reflects motion. Its value may range from a few to about 100 kHz. Very recently Iijima et al.[47] demonstrated on solid paramagnetic samples that separation of the quadrupole and paramagnetic tensors is possible by a 2D ^{2}H NMR method using strong radio frequency (rf) pulses. The ^{2}H MAS spectra can provide essential information about hydrogen bonding too. Chiba already found long ago[48a] that deuterons that take part in short, strong hydrogen bonds have smaller ^{2}H C_Q values than those forming weak hydrogen bonds. Furthermore, significant rhombicity in the quadrupolar tensor is observed in compounds with strong hydrogen bonds.[48b] More recently Zhao et al.[49] confirmed this correlation by *ab initio* calculations. Webber and Penner[50] studied the problem of inequivalent hydrogen bonds very recently using a combined experimental and quantum chemical approach and found that the quadrupolar tensor asymmetry parameter η_Q also depends on the geometry of hydrogen bonds (the larger its value, the more linear the bond). For instance, the Cu−N−D valence angles may depend on the geometry of hydrogen bonds, and thus affect two-bond hyperfine couplings. It is also noteworthy that, as already pointed out in the Theory section, the ^{2}H line width is often smaller that of the ^{1}H due to its smaller γ value.[14]

3.2. Exchangeable Deuterons: ^{2}H Fast-MAS Experiments on Amine Deuterated Complexes. 3.2.1. Bis([D$_2$]alaninato)-copper(II) Complexes. To further validate the assignment of the *cis* and *trans* isomers and to gain insight into the internal dynamics we recorded the ^{2}H fast-MAS spectra of several polydeuterated (D$_4$, D$_8$) or perdeuterated (D$_{12}$) bis(alaninato)-copper(II) complexes. The ^{2}H data are collected in Table 2.

Originally Lui et al. reported[14] the ^{2}H MAS spectra of the selectively deuterated aqua D,L **1a** (ee). Later *trans* configuration was confirmed by X-ray crystal structures.[17a−d] Our ^{2}H MAS spectra obtained for amine-deuterated D$_4$ forms of *trans* **1a**, *cis* **1a**, and **1b** are shown in Figure 6. As revealed by the inspection of the spinning sideband manifolds (for the complete spectrum see Supporting Information Figure S7) the sideband intensities were only slightly asymmetric, which indicated that the electron−^{2}H dipolar interaction is small.[15] The relevant Cu-to-D distances were about 2.5−2.7 Å.[17a−d,18a−c] Only two low-frequency shifted signals were seen in the spectrum (due to the negative two-bond FC contribution) of the *trans* D,L aqua complex (Figure 2, middle). The obtained shifts were very close to the reported data[14] of the aqua D,L-D$_{12+2(water)}$ (ee) form (Table 2). Furthermore, the water deuterons were invisible on our room-temperature spectrum, which is also in agreement with the previously reported spectrum.[14] Our C_Q and η_Q values (Table 2) agree reasonably well with the values reported by Lee et al. (C_Q = 190 kHz, η_Q = 0.2).[15]

In the spectrum of the anhydrous L,L isomer **1b** (Table 2 and Figure 6, top), in agreement with the C_1 symmetry proposed above on the basis of ^{13}C MAS spectra, four different ND sites were observed. It is noteworthy that two of them were very close to those observed in the *trans* D,L isomer (Figure 4, middle). We know that in the D,L isomer the methyls are in the equatorial positions; thus, it is tempting to also assume *trans* arrangement of the ligands in the L,L complex, and to assign the ND signals at −124.0 and −150.5 ppm to the ligand with equatorial methyl and the other two to the other ligand with axial methyl group.

Table 2. ^{2}H MAS Chemical Shift δ_p (ppm), DFT/B3LYP δ_{FC}^{calcd} (ppm), Motion-Averaged Quadrupolar Coupling C_Q (kHz), and Quadrupolar Tensor Asymmetry η_Q Values of the Studied Amine-Deuterated D$_2$ Complexes *trans* 1a, *cis* 1a, *trans* 1b, 2, 3, and 4^a

deuterium	δ_p	δ_{FC}^{calcd}	C_Q	η
		1a *trans* (ee)		
ND (a)	−127.6		191	0.10
ND (e)	−153.0		193	0.15
		1a *cis* (aa)		
ND (a)	−117.3		∼190−210	∼0.10−0.00
ND (e)	−154.2		∼190−210	∼0.15−0.00
		1b *trans* (ea)		
ND (a)	−103.9		∼210	∼0.00
ND (e)	−124.0		∼210	∼0.00
ND′ (a)	−143.9		∼210	∼0.00
ND′ (e)	−150.5		∼210	∼0.00
		2		
ND (a)	−125.1	−167	200	0.25
ND (e)	−154.4	−196	207	0.20
		3		
ND (a)	−122.8	−145	196	0.05
ND (e)	−144.0	−169	186	0.20
		4		
ND (a)	−113.2		187	0.23
ND (e)	−160.0		187	0.23

^{a}The assignments of the ND deuterons to the axial (a) and equatorial (e) positions of the chelate rings are based on the O−Cu−N−D torsional angles and are tentative only.

The spectrum of the suspected mixture of the metastable *cis* (D,L; D,D; L,L; L,D) isomers (Figure 6, bottom) also exhibited two signals. Therefore, this complex must have 2-fold symmetry too. Apart from the relative heights, the signals were similar to those of the *trans* D,L form (Figure 6, middle). Only nearly identical and dominant two-bond FC contributions can explain this. Remember that the ^{13}C MAS spectra of the *trans* D,L form and the metastable *cis* sample were different (see Figure 3, middle and bottom); their difference was explained by the different methyl configurations (aa) and (ee). Data obtained from the known *cis* and *trans* single-crystal structures[17a−d,18a−c] indicate that the Cu−N−D distances and valence angles are indeed similar (the deviations are ±0.01 Å and ±1.5°, respectively). A thorough inspection of the available experimental crystal structures also revealed that in the *trans* D,L (ee) isomer the coordination plane was irregular square-planar but in the *cis* and *trans* L,L (ae) isomers the copper(II) coordination was distorted planar (e.g., in the *cis* isomer[18c] the *trans* O−Cu−N angles are ∼175° and −177°). It seems that the impact of the (a) or (e) neighboring methyl group on Cu-to-D distances and/or Cu−N−D valence angles, and therefore on the PCS and two-bond FC contributions, is practically negligible.

Line shape simulations[33] (accounting only for the quadrupolar tensor) of the ND signals of the *cis* isomer resulted in rather large residual C_Q and indicated near axial symmetry of η_Q for all signals (Table 2). These data suggest the presence of static amine deuterons not related by symmetry.

3.2.2. Bis([D$_2$]1-amino(cyclo)alkane-1-carboxylato-κ^2N,O)-copper(II) Complexes. Only two low-frequency ND signals were observed in ^{2}H MAS spectra of amine-deuterated complexes **2**, **3**, and **4**, but not **5** (Figure 7, Table 2), which is in agreement with the symmetry suggested by the ^{13}C MAS
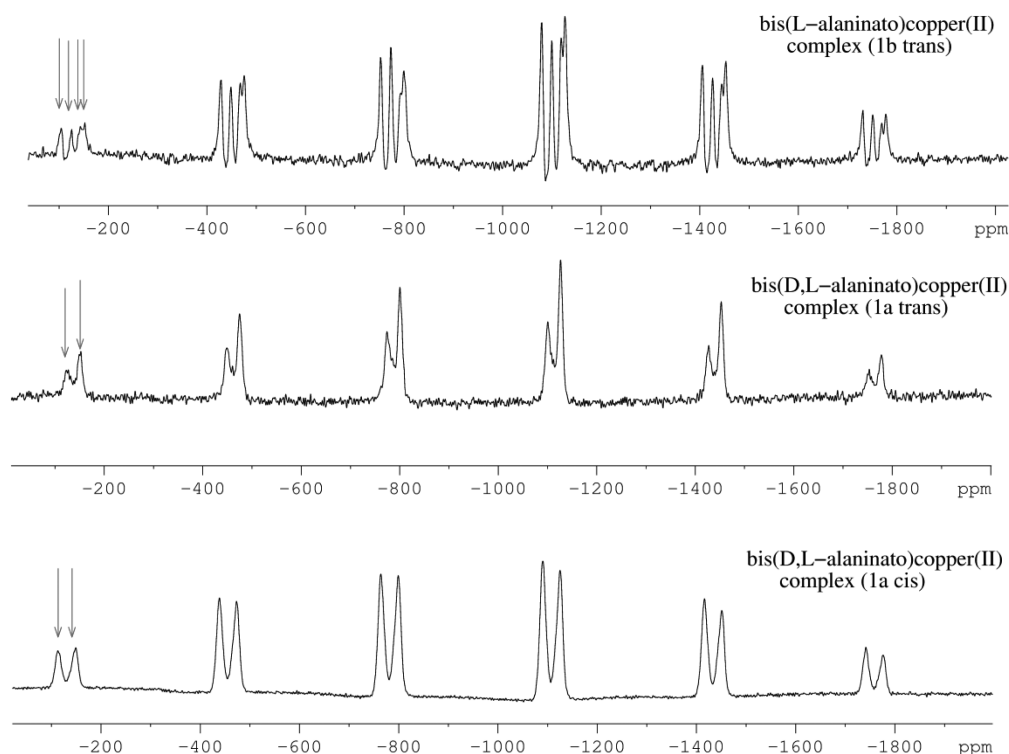
Figure 6. Comparison between the ^{2}H fast-MAS spectra of the bis([D_2]alaninato)copper(II): aqua D,L isomer (**1a** *trans*, middle), the anhydrous L,L isomer (**1b** *trans*, top), and the suspected mixture of *cis* (D,L; D,D; L,L; L,D) isomers (**1a** *cis*, bottom). 61.42 MHz, rotation 20 kHz. The isotropic signals are indicated by arrows; in addition, five low-frequency SSBs are also shown.
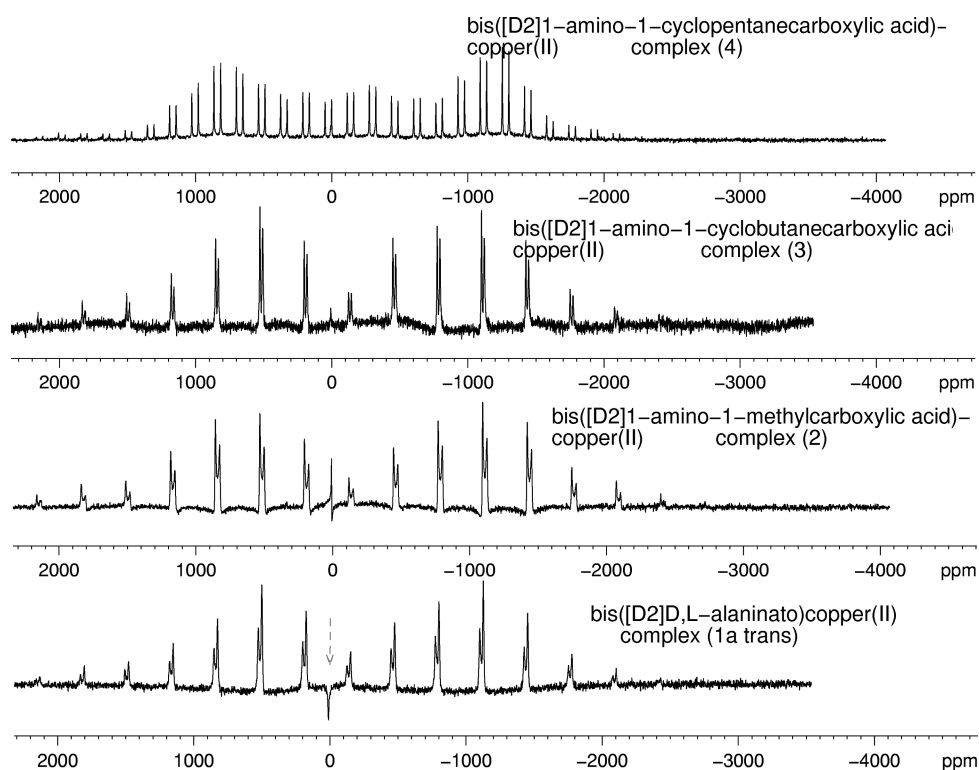

Figure 7. Comparison of solid-state ^{2}H fast-MAS spectra of ND$_2$ forms of complexes *trans* **1a** 20 kHz, **2** 20 kHz, **3** 20 kHz, and **4** 10 kHz. Whole spectra, 61.42 MHz, 2.5 mm rotor, room temperature ~300 K. The dotted arrow line indicates an artifact (the carrier frequency).

(Table 1) and X-ray diffraction results.[17a,19a,b,20] Not surprisingly, the observed ^{2}H ND chemical shifts of **2** were very close to those of **1a**. The ^{2}H ND shift values obtained for **3** were also similar to those of **2**. Remember that both **2** and **3** have a center of inversion. In **3** the Cu−N−D valence angles obtained from the X-ray structure[20] were 110 ± 0.2° for both deuterons. Therefore, the observed 21−22 ppm chemical shift difference of the two deuterium sites (in the five-membered
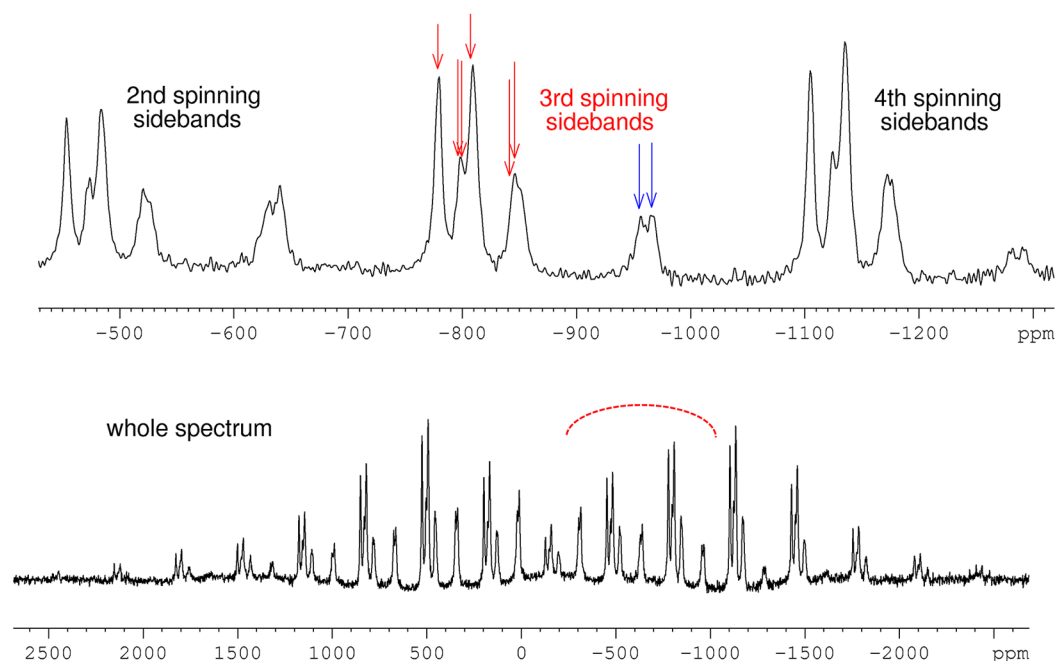
Figure 8. ^{2}H fast-MAS spectrum of the ND$_2$ form of **5**. Top: extension, second to fourth low-frequency spinning sidebands. The red and blue arrows indicate the third spinning sidebands of the ND and OD deuterons, respectively. Bottom: whole spectrum. Larmor frequency 61.42 MHz, rotation 20 kHz, 2.5 mm rotor, 300 K.

Table 3. ^{2}H Paramagnetic Shifts δ_P's (ppm), Relative Signal Intensities, Quadrupolar Coupling Values C_Q's (kHz), Asymmetry Parameters η_Q's, Cu−N−H Valence Angles (deg) from the X-ray Crystal Structure,[20] and DFT/B3LYP δ_{FC}^{calcd}'s (ppm) of the *cis−trans* Dimer in **5**[a]

	ND deuterons						OD deuterons	
	cis	*trans*	*trans*	*trans*	*cis*	*cis*		
δ_P	−128.8	−147.4	−150.1	−159.5	−196.3	−201.7	19.8	10.2
intensity	2	1	1	2	1	1		
C_Q	187	197	197	199	203	203	100	105
η_Q	0.28	0.43	0.43	0.47	0.45	0.45	~1	~1
Cu−N−H	116.2	105.4	110.2	109.4	100.5	98.2		
	114.3			109.4				
δ_{FC}^{calcd}	−140	−163	−201	−166	−219	−231	−4	−1
	−150			−167				

[a]The signal assignment to either *cis* or *trans* isomer is based on the assumption that the FC term depends on the Cu−N−D valence angles (it is assumed that the Cu−N−D values do not differ significantly from the Cu−N−H values). The accuracy of the angles is limited by the ill-defined position of protons.

chelate rings these deuterons take axial and equatorial positions) can hardly be explained by intramolecular causes even if we take into account the location error for the protons. It is noteworthy that the low-frequency signal [−144 ppm, ND (e)] has a smaller C_Q value and a larger η_Q value than ND (a) (Table 2). We consider these results as possible indications for hydrogen-bond involvement.[46]

The largest chemical shift difference (∼56.8 ppm) between the amine deuterons was found in the cyclopentyl derivative **4** (Figure 7, Table 2). The reason is unclear. Values of the obtained quadrupolar coupling constants and paramagnetic shift tensor asymmetry parameters proved static ND deuterons in all complexes.

The situation was quite different with complex **5**. Eight different ND deuterium sites were expected in the *cis−trans* dimer with C_1 symmetry. In the ^{2}H MAS spectrum, apart from

the two signals of the D$_2$O molecules, only six different sites were observed (Figure 8 and Table 3) but with 2:1:1:2:1:1 intensity ratios; i.e., there were two overlaps. The experimental Cu−N−D valence angles (Table 3) could be correlated with the size of the FC contribution by a quadratic function (Supporting Information Figure S12). The X-ray crystal structure showed two identical Cu−N−D angles and another similar angle pair (114.2°, 116.2°).[20] Also note that the X-ray structure analysis[20] did not produce very accurate positions for hydrogen atoms. In addition, the observed ^{2}H line widths were about 7 ppm (∼420 Hz) wide.

The C_Q and η_Q values (Table 3) clearly suggest motionally rigid ND deuterons taking part in hydrogen bonds. Indeed, the X-ray structure shows that they form hydrogen bonds to the carbonyl oxygen atoms of the neighboring complexes. In

Table 4. Collected ^{2}H Isotropic Chemical Shifts δ_p (ppm), Estimates of Motionally Averaged Quadrupolar Coupling C_Q (kHz), Quadrupolar Tensor Asymmetry η, and Hyperfine Coupling A of Available Deuterated Forms of Bis([D$_n$]alaninato)copper(II) Complexes (n = 4, 8, 12) *trans* 1a , *cis* 1a, and *trans* 1b[a]

[D$_n$] form; D nuclei	δ_p	C_Q	η
	1a *trans* (ee)		
[D$_4$]; N,N′D$_2$ ($A_2 < 0$)	−127.6, −153.0	191[b], 193[b]	0.10, 0.15
	−132.7,[c] −159.5[c]	190[c]	0.20[c]
[^{15}N][D$_4$];[e] N,N′D$_2$ ($A_2 < 0$)	−128.3, −155.4	193, 192	0.15, 0.10
[D$_{12}$]; N,N′D$_2$ ($A_2 < 0$)	−130.6[c], −159.0[c]		
[D$_{12}$]; C2,2′D ($A_3 > 0$)	8.4[c], 0[d]		
[D$_{12}$]; C3,3′D$_3$ ($A_4 > 0$)	32.0[c], 20.4[c], 34[d]		
	1a *cis* (aa)		
[D$_4$]; N,N′D$_2$ ($A_2 < 0$)	−117.3, −154.2	190−210	0.10−0.00, 0.15−0.00
	1b *trans* (ae)		
[D$_4$]; ND$_2$ ($A_2 < 0$)	−103.9, −124.0	∼210	∼0.00
[D$_4$]; N′D$_2$ ($A_2 < 0$)	−143.9, −150.5	∼210	∼0.00
[D$_8$]; C2,2′D ($A_3 > 0$)	103.7, 48[d] (e)	156 (e)	0.01 (e)
	32.8, 67[d] (a)	167 (a)	0.01 (a)
[D$_8$]; C3,3′D$_3$ ($A_4 > 0$)	41.5, 31[d] (e)	54 (e)	0.30 (e)
	9.6, 3[d] (a)	52 (a)	0.37 (a)
[D$_{12}$]; ND$_2$ ($A_2 < 0$)	−104.3, −125.1	206, 211	0.00
[D$_{12}$]; N′D$_2$ ($A_2 < 0$)	−141.1, −149.3	207, 200	0.00
[D$_{12}$]; C2,2′D ($A_3 > 0$)	100.1 (e)	155 (e)	0.17 (e)
	31.7 (a)	147 (a)	0.16 (a)
[D$_{12}$]; C3,3′D$_3$ ($A_4 > 0$)	40.1 (e)	59 (e)	0.12 (e)
	9.2 (a)	55 (a)	0.12 (a)

[a]The signal assignment to the axial and equatorial chelate-ring conformations [denoted with (a) and (e), respectively] was based on the assumption of a Karplus-like dihedral angle dependence of the three-bond Cu−N−C−D hyperfine couplings [the average values of the Cu−N−C−D dihedral angles obtained from the reported single-crystal structures[17a,18a,b] are 135 ± 5° in (e), and 85−95° in (a)]. [b]Results of simulations based solely on the quadrupolar interaction.[33] [c]Reference 14. [d]Results of the DFT/B3LYP calculations (Supporting Information Table S1; the average value used for the CD$_3$ groups). [e]Data obtained for the ^{15}N labeled compound are included only to show the reproducibility of the experimental values on different samples (crystals).

contrast, the OD deuterons, as indicated by their much smaller C_Q and large η_Q values, are much less rigid in the crystal lattice.

3.3. Nonexchangeable Deuterons: ^{2}H Fast-MAS Experiments on the Bis([D$_n$]alaninato)copper(II) Complexes: D$_8$ (Aliphatic Only) and D$_{8+4(amine)=12}$ (Perdeuterated) Aqua Forms, Identification of D,L and L,L Isomers. To further validate the assignment of the D,L and L,L isomers and to gain insight into the internal dynamics of these complexes we recorded the ^{2}H fast-MAS spectra of several polydeuterated (D$_4$, D$_8$) and/or perdeuterated (D$_{12}$) bis(alaninato)copper(II) complexes (Table 4).

Literature data exist for the D$_8$ form of the aqua *trans* D,L but not for the L,L isomer. Three signals have been found for the aqua D,L isomer at 32.0 (CD$_3$), 20.4 (CD$_3$), and 8.4 ppm (CD).[14] However, no reasoning was given for the presence of two signals of very different intensities and their assignment to the CD$_3$ deuterons.[14] Different intensities of the isotropic signals can be the consequence of different anisotropy and asymmetry of the quadrupolar tensors; however, this interpretation is unreasonable for two similarly rotating methyl groups in the molecule with 2-fold symmetry, as indicated by the ^{13}C MAS spectra.[4]

Assignments of the ND$_2$, C2,2′D, and C3,3′D$_3$ deuterons were possible on the basis of the simulated motionally averaged C_Q values and the expected sign and magnitude of the dominant FC contribution. Both the three-bond (C2,2′D) and four-bond (C3,3′D) FC contributions are positive, but as expected, the magnitude of the latter one is much smaller.[2]

In *trans* **1b**, unambiguous assignment of the signals to either axial or equatorial chelate-ring atoms was not possible for the nitrogen and methyl (C3,3′) bound deuterons. In cases of deuterons bound to the C2,2′ carbons the axial and equatorial descriptions were assigned again assuming a Karplus-like dihedral angle dependence[2] of the three-bond Cu−N−C−D hyperfine couplings (Supporting Information Figure S11). On this basis the signals at 103.7 and 32.8 ppm (see data of complex **1b** in Table 4) were assigned to the equatorial and axial positions, respectively.

The 1D spectrum of the *trans* L,L-D$_8$ form is well-resolved, and the quadrupolar line shape is near symmetrical (Figure 9 (bottom) and Supporting Information Figure S7). It is clear that the ligands' conformations are different, so the complex lacks symmetry, which is in agreement with the ^{13}C data (see Figure 1, top). Note that both the sensitivity and the resolution of the ^{2}H MAS spectrum were superior to those of the ^{13}C MAS spectra. Shifts of the CD$_3$ and CD deuterons agree well with the reported ^{1}H data[5] (Supporting Information Figure S8). Figure 9 illustrates the rapidly disappearing SSB intensities of the methyl deuterons relative to those of the methine deuterons in a comparison of the second and third spinning sidebands.

The obtained C_Q and η_Q (Table 4) indicate that while the CD deuterons are static the deuterons of the CD$_3$ groups are possibly involved in a three-site fast jumping process[45] [C_Q (motionally averaged) = 52−59 kHz]. Shi et al.[51] reported that the C_Q and η_Q values of the U-[^{2}H$_4$/^{13}C$_3$/^{15}N]-alanine were 155 kHz/0.0 and 160 kHz/0.0 for the unaveraged quadrupolar
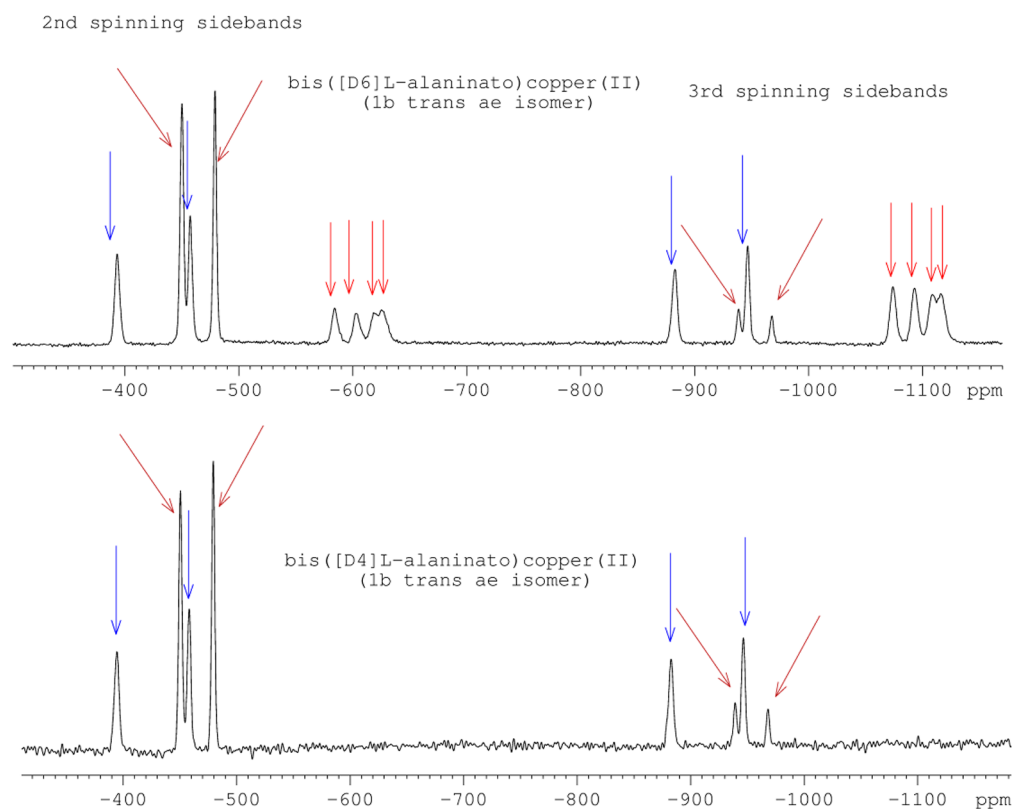
Figure 9. Comparison between ^{2}H MAS spectra of the *trans* L,L-D$_8$ (bottom) and *trans* L,L-D$_{8+4=12}$ (top) forms of the L-alaninato complex (**1b**). Only the low-frequency second and third SSBs are shown for clarity. The N,N′D$_2$, C2,2′D, and C3,3′D$_3$ signals are indicated by red, blue, and tilted brown arrows, respectively. Larmor frequency 61.42 MHz, rotation speed 30 kHz, sample temperature 300 K. The total acquisition time was about 5 min.

tensor of the rotating methyl deuterons (using a three-site jump model)[52] and for the static methine deuteron,[53] respectively, which is in agreement with our findings.

In the spectrum of the *trans* L,L-D$_{12}$ complex (Table 4, Figure 9, top) four additional low-frequency shifted signals were detected (indicated by red arrows). They can be assigned to the different ND deuteron sites. The C_Q and η_Q values of the quadrupolar tensors calculated for them are very similar to those of the ND deuterons of the *trans* L,L-D$_4$ complex (Table 2).

CONCLUSIONS

In agreement with earlier reports[4−11] we confirmed that recording of good quality NMR spectra of paramagnetic Cu(II) complexes can be faster in solids than in solution state due mainly to their favorable T_{1z}, T_{1Q}, and T_2 relaxation properties. Furthermore, the paramagnetic effects add to the chemical shift differences existing in diamagnetic complexes making resolution better and, thus, identification of stereoisomers easier. Bis(alaninato)copper(II) complexes were studied in detail, and we have shown that both ^{13}C and ^{2}H MAS spectra can distinguish between the D,L (diaxial or diequatorial) and L,L (axial−equatorial) diastereomers of bis([D$_n$]alaninato)copper-(II) (n = 0, 2, 8) complexes primarily owing to the different FC contributions. The three-bond hyperfine couplings clearly show Karplus-like dependence ($f(\cos^2\theta)$) on the Cu−N−C2−C3 or Cu−N−C2−D torsional angles which turns out to be a useful assignment aid. At the same time the FC term is remarkably less sensitive to the *cis* or *trans* CuN$_2$O$_2$ configuration in the studied complexes. Therefore, *a priori* identification of the coordination mode is not possible from the NMR spectra

alone. Crystal structures and DFT/B3LYP calculations were also used to complement the final assignments. The correlations obtained for bis(alaninato-$\kappa^2 N,O$)copper(II) complexes were successfully used to characterize the stereochemistry of analogous bis(1-amino(cyclo)alkane-1-carboxylato-$\kappa^2 N,O$)copper(II) complexes (**2−4**). Even in the case of the double-sized *cis−trans* dimer (**5**), both the ^{13}C and ^{2}H (ND) resolutions were good enough to confirm the presence of two different complexes in the asymmetric unit.

Even though deuteration of molecules of interest may be expensive and tiresome, note that chances of routine measurements at natural abundance are steadily increasing.[54] Even spectra of the easily exchangeable amine protons (i.e., those of the bis-D$_2$ forms) contained a lot of essential stereochemical information. With regard to the internal solid-state motions going on in the crystal lattice of these molecules, the obtained quadrupolar tensor parameters were similar for the D,L and L,L alaninato isomers and also for the *cis−trans* forms. The obtained C_Q values suggest static amine deuterons with hydrogen-bond involvement in all complexes, and fast rotating methyl groups (similar crystal packing effects) in *trans* **1b**.

ASSOCIATED CONTENT

Ⓢ Supporting Information

General methodological remarks on ssNMR spectroscopy and the fast-MAS method. Rotation rate dependence of the ^{13}C MAS spectra (Figure S1), collection of ^{13}C CPMAS spectra of the free crystalline ligands (Figure S2), comparison of ^{13}C CPMAS spectra of the polycrystalline complexes and the free ligands (Figures S3−S6). ^{1}H and ^{2}H fast-MAS spectra of the Cu(II)([D$_4$]L-alanine)$_2$ complex (Figures S7−S8). Details of

the DFT/B3LYP calculations, ^{13}C and ^1H spin densities, and δ_{FC}^{calcd} of the cluster systems of *trans* **1b**, *cis* **1b**, *trans* **1a** hydrate, *cis* **1a** hydrate (Table S1); 17-Cu cluster model generated from MM predicted crystal structure of **1a** *cis* hydrate (Figure S9); ^{13}C and ^1H spin densities, and δ_{FC}^{calcd} for complexes **2**, **3**, and **4** (Table S2). ^{13}C and ^1H spin densities, δ_{FC}^{calcd}, δ_{dia}^{calcd}, and $\delta_{complex}^{calcd}$ for complex **5** (Table S3); correlations between the experimental and calculated shift values of the C3,3′ atoms (Figure S10); gas and solution phase DFT/B3LYP relative energies of the **1a** and **1b** stereoisomers (Table S4). Karplus dependence of the FC values on the dihedral angles (Figure S11) and quadratic dependence of the FC values on Cu−N−D valence angles (Figure S12) in complex **5**. This material is available free of charge via the Internet at http://pubs.acs.org.

■ AUTHOR INFORMATION

Corresponding Author

*E-mail: Szalontai.Gabor@solidnmr.hu. Phone: +36 88 624356.

Notes

The authors declare no competing financial interest.

■ REFERENCES

(1) (a) Harris, R. K. Crystallography and NMR: An Overview. In *Encyclopedia of Magnetic Resonance*; John Wiley and Sons, Ltd.: Chichester, U.K., 2008; pp 1−13. (b) Bhaumik, A.; Luchinat, C.; Parigi, G.; Ravera, E.; Rinaldelli, M. *CrystEngComm* **2013**, *15*, 8639−8656 and references cited therein. (c) Kervern, G.; D'Aléo, A.; Toupet, L.; Maury, O.; Emsley, L.; Pintacuda, G. *Angew. Chem., Int. Ed.* **2009**, *48*, 3082−3086.

(2) (a) Bertini, I.; Luchinat, G.; Parigi, G. Solution NMR of Paramagnetic Molecules. In *Current Methods in Inorganic Chemistry*; Elsevier: Amsterdam, 2001. (b) Kervern, G.; Pintacuda, G.; Zhang, Y.; Oldfield; Rcukoss, C.; Kuntz, E.; Herdtweck, E.; Basset, J.-M.; Cadars, S.; Lesage, A.; Copéret, C.; Emsley, L. *J. Am. Chem. Soc.* **2006**, *128*, 13545−13552. (c) Clément, R. J.; Pell, A. J.; Middlemiss, D. S.; Strobridge, F. C.; Miller, J. K.; Whittingham, M. S.; Emsley, L.; Pintacuda, G. *J. Am. Chem. Soc.* **2012**, *134*, 17178−17185. (d) Pell, A. J.; Pintacuda, G. *Prog. Nucl. Magn. Reson. Spectrosc.* **2015**, *84−85*, 33−72.

(3) Aime, S.; Bertini, I.; Luchinat, C. *Coord. Chem. Rev.* **1996**, *150*, 221−242.

(4) Ishii, Y.; Wickramashinghe, N. P.; Chimon, S. *J. Am. Chem. Soc.* **2003**, *125*, 3438−3439.

(5) Wickramashinghe, N. P.; Shaibat, M. A.; Ishii, Y. *J. Am. Chem. Soc.* **2005**, *127*, 5796−5797.

(6) Shaibat, A.; Casablanca, L. B.; Wickramashinghe, N. P.; Guggenheim, S.; de Dios, A. C.; Ishii, Y. *J. Am. Chem. Soc.* **2007**, *129*, 10968−10969.

(7) Wickramashinghe, N. P.; Shaibat, M. A.; Ishii, Y. *J. Phys. Chem. B* **2007**, *111*, 9693−9696.

(8) Wickramashinghe, N. P.; Shaibat, M. A.; Jones, C. H.; Casabianca, L. B.; de Dios, A. C.; Harwood, J. S.; Ishii, Y. *J. Chem. Phys.* **2008**, *128*, 052210/1−052210/15.

(9) Wickramashinghe, N. P.; Ishii, Y. *J. Magn. Reson.* **2006**, *181*, 233−243.

(10) Kumara Swamy, S.; Karczmarska, A.; Makowska-Janusik, M.; Kassiba, A.; Dittmer, J. *ChemPhysChem* **2013**, *14*, 1864−1870.

(11) Szalontai, G.; Sabolović, J.; Marković, M.; Balogh, Sz. *Eur. J. Inorg. Chem.* **2014**, 3330−3340.

(12) Schmidt-Rohr, K.; Spiess, H. W. *Multidimensional Solid-State NMR and Polymers*; Academic Press: London, 2004.

(13) Duer, M. J. *Introduction to Solid-State NMR Spectroscopy*; Blackwell Publishing: Oxford, U.K., 2004.

(14) Liu, K.; Ryan, D.; Nakanishi, K.; McDermott, A. *J. Am. Chem. Soc.* **1995**, *117*, 6897−6906.

(15) Lee, H.; Polenova, T.; Beer, R. H.; McDermott, A. *J. Am. Chem. Soc.* **1999**, *121*, 6884−6894.

(16) Vega, A. J. Quadrupolar Nuclei in Solids. In *Solid-State NMR Studies of Biopolymers*; McDermott, A. E.; Polenova, T., Eds.; John Wiley & Sons Ltd.: Chichester, U.K., 2010; pp 111−138.

(17) (a) Hitchman, M. A.; Kwan, L.; Engelhardt, L. M.; White, A. H. *J. Chem. Soc., Dalton Trans.* **1987**, 457−465. (b) Mirceva, A.; Thomas, J. O.; Gustafsson, T. *Acta Crystallogr., Sect. C* **1989**, *45*, 1141−1144. (c) Calvo, R.; Levstein, P. R.; Castellano, E. E.; Fabiane, S. M.; Piro, O. E.; Oseroff, S. B. *Inorg. Chem.* **1991**, *30*, 216−220. (d) Zhang, Y.; Sun, H.; Oldfield, E. *J. Am. Chem. Soc.* **2005**, *127*, 3652−3653. (e) O'Brien, P. *J. Chem. Educ.* **1982**, *59*, 1052−1053.

(18) (a) Dijkstra, A. *Acta Crystallogr.* **1966**, *20*, 588−590. (b) Blazic, B.; Bukovec, N.; Bukovec, P.; Lazarini, F. *Vestn. Slov. Kem. Drus.* **1992**, *39*, 285−290. (c) Moussa, S. M.; Fenton, R. R.; Kennedy, B. J.; Piltz, R. O. *Inorg. Chim. Acta* **1999**, *288*, 29−34.

(19) (a) Calvo, R.; Mesa, M. A.; Oliva, G.; Zukerman-Schpector, J.; Nascimento, O. R.; Tovar, M.; Arce, R. *J. Chem. Phys.* **1984**, *81*, 4584−4591. (b) Oliva, G.; Castellano, E. E.; Zukerman-Schpector, J.; Calvo, R. *Acta Crystallogr.* **1986**, *C42*, 19−21.

(20) Góger, Sz.; Pap, J. S.; Bogáth, D.; Simaan, A. J.; Speier, G.; Giorgi, M.; Kaizer, J. *Polyhedron* **2014**, *73*, 37−44.

(21) Harris, R. K. *Solid State Sci.* **2004**, *6*, 1025−1037.

(22) (a) Kaupp, M.; Köhler, F. H. *Coord. Chem. Rev.* **2009**, *253*, 2376−2386. (b) Ashbrook, S. E.; Dawson, D. M. *Acc. Chem. Res.* **2013**, *46*, 1964−1974.

(23) (a) Wilkens, S. J.; Xia, B.; Weinhold, F.; Markley, J. L.; Westler, W. M. *J. Am. Chem. Soc.* **1998**, *120*, 4806−4814. (b) Carlier, D.; Ménétrier, M.; Grey, C. P.; Delmas, C.; Ceder, G. *Phys. Rev. B: Condens. Matter Mater. Phys.* **2003**, *67*, 174103/1−174103/14. (c) Vaara, J. *Phys. Chem. Chem. Phys.* **2007**, *9*, 5399−5418. (d) Pennanen, T. O.; Vaara, J. *Phys. Rev. Lett.* **2008**, *100*, 133002/1−133002/4. (e) Middlemiss, D. S.; Ilott, A. J.; Clément, R. J.; Strobridge, F. C.; Grey, C. P. *Chem. Mater.* **2013**, *25*, 1725−1734.

(24) *Calculation of NMR and EPR Parameters: Theory and Applications*; Kaupp, M., Bühl. M., Malkin, V. G., Eds.; Wiley-VCH: Weinheim, 2004.

(25) (a) Charnock, G. T. P.; Kuprov, I. *Phys. Chem. Chem. Phys.* **2014**, *16*, 20184−20189. (b) Koehler, J.; Meiler, J. *Prog. Nucl. Magn. Reson. Spectrosc.* **2011**, *59*, 360−389. (c) Bertini, I.; Luchinat, C.; Parigi, G. *Prog. Nucl. Magn. Reson. Spectrosc.* **2002**, *40*, 249−273. (d) Nayeem, A.; Yesinowski, J. P. *J. Chem. Phys.* **1988**, *89*, 4600−4608. (e) Brough, A. R.; Grey, C. P.; Dobson, C. M. *J. Am. Chem. Soc.* **1993**, *115*, 7318−7327.

(26) Jaroniec, C. P. *Solid State Nucl. Magn. Reson.* **2012**, *43−44*, 1−13.

(27) Kubo, A.; Spaniol, T. P.; Terao, T. *J. Magn. Reson.* **1998**, *133*, 330−340.

(28) Bryce, D. L.; Bernard, G. M.; Gee, M.; Lumsden, M. D.; Euchele, K.; Wasylishen, R. E. *Can. J. Anal. Sci. Spectrosc.* **2001**, *46*, 46−82.

(29) (a) Solomon, I. *Phys. Rev.* **1955**, *99*, 559−565. (b) Bloembergen, N. *Chem. Phys.* **1957**, *27*, 572−573. (c) Kervern, G.; Steuernagel, S.; Engelke, F.; Pintacuda, G.; Emsley, L. *J. Am. Chem. Soc.* **2007**, *129*, 14118−14119. (d) Bakhmutov, V. *Chem. Rev.* **2011**, *111*, 530−562.

(30) Calvo, R.; Passegi, M. C.; Novak, M. A.; Symko, O. G.; Oseroff, S. B.; Nascimento, O. R.; Terrile, M. C. *Phys. Rev. B* **1991**, *43*, 1074−1083.

(31) Stejkal, E. O.; Memory, J. D. *High Resolution NMR in the Solid State*; Oxford University Press: Oxford, U.K., 1994.

(32) Wu, X.; Burns, S. T.; Zilm, K. W. *J. Magn. Reson., Ser. A* **1994**, *111*, 29−36.

(33) Bruker BioSpin software. *Topspin 2.1.3*.

(34) Macho, V.; Brombacher, L.; Spiess, H. W. *Appl. Magn. Reson.* **2001**, *20*, 405−432.

(35) (a) Becke, A. D. *J. Chem. Phys.* **1993**, *98*, 5648−5652. (b) Lee, C.; Yang, W.; Parr, R. G. *Phys. Rev. B* **1988**, *37*, 785−789. (c) Vosko, S. H.; Wilk, L.; Nusair, M. *Can. J. Phys.* **1980**, *58*, 1200−1211. (d) Stephens, P. J.; Devlin, F. J.; Chabalowski, C. F.; Frisch, M. J. *J. Phys. Chem.* **1994**, *98*, 11623−11627. (e) Wachters, A. J. H. *J. Chem. Phys.* **1970**, *52*, 1033−1036. (f) Cheeseman, J. R.; Trucks, G. W.; Keith, T. A.; Frisch, M. J. *J. Chem. Phys.* **1969**, *104*, 5497−5509.

(36) (a) Tomasi, J.; Mennucci, B.; Cancés, E. *THEOCHEM* **1999**, *464*, 211−226. (b) Cossi, M.; Scalmani, G.; Rega, N.; Barone, V. *J. Chem. Phys.* **2002**, *117*, 43−54. (c) Adamo, C.; Scuseria, G. E.; Barone, V. *J. Chem. Phys.* **1999**, *111*, 2889−2899. (d) Adamo, C.; Barone, V. *J. Chem. Phys.* **1999**, *110*, 6158−6170. (e) Adamo, C.; Cossi, M.; Scalmani, G.; Barone, V. *Chem. Phys. Lett.* **1999**, *307*, 265−271.

(37) Frisch, M. J.; Trucks, G. W.; Schlegel, H. B.; Scuseria, G. E.; Robb, M. A.; Cheeseman, J. R.; Montgomery, J. A.; Vreven, T., Jr.; Kudin, K. N.; Burant, J. C.; Millam, J. M.; Iyengar, S. S.; Tomasi, J.; Barone, V.; Mennucci, B.; Cossi, M.; Scalmani, G.; Rega, N.; Petersson, G. A.; Nakatsuji, H.; Hada, M.; Ehara, M.; Toyota, K.; Fukuda, R.; Hasegawa, J.; Ishida, M.; Nakajima, T.; Honda, Y.; Kitao, O.; Nakai, H.; Klene, M.; Li, X.; Knox, J. E.; Hratchian, H. P.; Cross, J. B.; Bakken, V.; Adamo, C.; Jaramillo, J.; Gomperts, R.; Stratmann, R. E.; Yazyev, O.; Austin, A. J.; Cammi, R.; Pomelli, C.; Ochterski, J. W.; Ayala, P. Y.; Morokuma, K.; Voth, G. A.; Salvador, P.; Dannenberg, J. J.; Zakrzewski, V. G.; Dapprich, S.; Daniels, A. D.; Strain, M. C.; Farkas, O.; Malick, D. K.; Rabuck, A. D.; Raghavachari, K.; Foresman, J. B.; Ortiz, J. V.; Cui, Q.; Baboul, A. G.; Clifford, S.; Cioslowski, J.; Stefanov, B. B.; Liu, G.; Liashenko, A.; Piskorz, P.; Komaromi, I.; Martin, R. L.; Fox, D. J.; Keith, T.; AL-Laham, M. A.; Peng, C. Y.; Nanayakkara, A.; Challacombe, M.; Gill, P. M. W.; Johnson, B.; Chen, W.; Wong, M. W.; Gonzalez, C.; Pople, J. A.; *Gaussian 03, revision E.01*; Gaussian, Inc.: Wallingford, CT, 2004.

(38) Sinker, J.; Seyfarth, L.; Voll, J. *Solid State Sci.* **2004**, *6*, 1039−1052.

(39) Karplus, M. *J. Am. Chem. Soc.* **1963**, *85*, 2870.

(40) Ma, L.; Jorgensen, A. M.; Sorensen, G. O.; Ulstrup, J.; Led, J. *J. Am. Chem. Soc.* **2000**, *122*, 9473−9485.

(41) Herlinger, A. W.; Wenhold, S. L.; Veach, T.; Long, I. I. *J. Am. Chem. Soc.* **1970**, *92*, 6474−6481.

(42) Rockenbauer, A. *J. Magn. Reson.* **1979**, *35*, 429−438.

(43) Pregosin, P. S.; Kunz, R. W. ^{31}P and ^{13}C NMR of Transition Metal Phosphine Complexes. In *NMR Basic Principles and Progress*; Diehl, P.; Fluck, E.; Kosfeld, R., Eds.; Springer Verlag: Berlin, 1979; Vol. *16*.

(44) (a) Sabolović, J.; Gomzi, V. *J. Chem. Theory Comput.* **2009**, *5*, 1940−1954. (b) Marković, M.; Judaš, N.; Sabolović, J. *Inorg. Chem.* **2011**, *50*, 3632−3644. (c) Marković, M.; Milić, D.; Sabolović, J. *Cryst. Growth Des.* **2012**, *12*, 4116−4129.

(45) (a) Brown, S. P. *Solid State Nucl. Magn. Reson.* **2012**, *41*, 1−27. (b) Kervern, G.; Pintacuda, G.; Emsley, L. *Chem. Phys. Lett.* **2007**, *435*, 157−162.

(46) Hologne, M.; Chevelkov, V.; Reif, B. *Prog. Nucl. Magn. Reson. Spectrosc.* **2006**, *48*, 216−232.

(47) Iijima, T.; Shimuzu, T.; Nishimura, K. *J. Magn. Reson.* **2015**, *251*, 57−64.

(48) (a) Chiba, T. *J. Chem. Phys.* **1964**, *41*, 1352−1358. (b) Hunt, M. J.; Mackay, A. L. *J. Magn. Reson.* **1974**, *15*, 402−414.

(49) Zhao, X.; Dvorak, M.; Silvernail, C.; Belot, J.; Harbison, G. *Solid State Nucl. Magn. Reson.* **2002**, *22*, 363−372.

(50) Webber, R.; Penner, G. H. *Solid State Nucl. Magn. Reson.* **2012**, *47−48*, 10−18.

(51) Shi, X.; Yarger, J. L.; Holland, G. P. *J. Magn. Reson.* **2013**, *226*, 1−12.

(52) Vold, R. L.; Hoatson, G. L. *J. Magn. Reson.* **2009**, *198*, 57−72.

(53) Veshtort, M.; Griffin, R. G. *J. Magn. Reson.* **2006**, *178*, 248−282.

(54) Lesot, P.; Courtieu, J. *Progress in Nuclear Magnetic Resonance Spectroscopy* **2009**, *55*, 128−159.